










Global Distribution of Key Features of Streamer Corona Discharges in Thunderclouds

S. Soler¹ , F. J. Gordillo-Vázquez¹ , F. J. Pérez-Invernón¹ , A. Luque¹ , D. Li² , T. Neubert² , O. Chanrion² , V. Reglero³, J. Navarro-González³ , and N. Østgaard⁴ 

¹Instituto de Astrofísica de Andalucía (IAA-CSIC), Glorieta de la Astronomía s/n, Granada, Spain, ²National Space Institute, Technical University of Denmark (DTU Space), Kongens, Denmark, ³Image Processing Laboratory, University of Valencia, Valencia, Spain, ⁴Department of Physics and Technology, Birkeland Centre for Space Science, University of Bergen, Bergen, Norway

Key Points:

- BLUEs are found between ~1 and ~4 km below cloud tops in the tropics and ≤1 km in mid and higher latitudes
- Two distinct populations of BLUEs with peak power density <25 μWm⁻² (common) and ≥25 μWm⁻² (rare) are observed
- Fast rise time (<0.05 ms) BLUEs occur very superficially (<1 km) near cloud tops with high power density ≥100 μWm⁻²

Supporting Information:

Supporting Information may be found in the online version of this article.

Correspondence to:

F. J. Gordillo-Vázquez,
vazquez@iaa.es

Citation:

Soler, S., Gordillo-Vázquez, F. J., Pérez-Invernón, F. J., Luque, A., Li, D., Neubert, T., et al. (2022). Global distribution of key features of streamer corona discharges in thunderclouds. *Journal of Geophysical Research: Atmospheres*, 127, e2022JD037535. <https://doi.org/10.1029/2022JD037535>

Received 21 JUL 2022

Accepted 5 DEC 2022

Author Contributions:

Conceptualization: S. Soler, F. J. Gordillo-Vázquez

Data curation: S. Soler

Formal analysis: S. Soler, F. J. Gordillo-Vázquez

Funding acquisition: F. J. Gordillo-Vázquez

Investigation: S. Soler, F. J. Gordillo-Vázquez, F. J. Pérez-Invernón, A. Luque, D. Li, T. Neubert, O. Chanrion, V. Reglero, J. Navarro-González, N. Østgaard

Visualization: S. Soler, F. J. Gordillo-Vázquez, F. J. Pérez-Invernón, A. Luque, D. Li, T. Neubert, O. Chanrion, V. Reglero, J. Navarro-González, N. Østgaard

© 2022 The Authors.

This is an open access article under the terms of the [Creative Commons Attribution-NonCommercial License](https://creativecommons.org/licenses/by/4.0/), which permits use, distribution and reproduction in any medium, provided the original work is properly cited and is not used for commercial purposes.

Abstract We present nighttime worldwide distributions of key features of Blue Luminous Events (BLUEs) detected by the Modular Multispectral Imaging Array of the Atmosphere-Space Interaction Monitor. Around 10% of all detected BLUEs exhibit an impulsive single pulse shape. The rest of BLUEs are unclear (impulsive or not) single, multiple or with ambiguous pulse shapes. BLUEs exhibit two distinct populations with peak power density <25 μWm⁻² (common) and ≥25 μWm⁻² (rare) with different rise times and durations. The altitude (and depth below cloud tops) zonal distribution of impulsive single pulse BLUEs indicate that they are commonly present between cloud tops and a depth of ≤4 km in the tropics and ≤1 km in mid and higher latitudes. Impulsive single pulse BLUEs in the tropics are the longest (up to ~4 km height) and have the largest number of streamers (up to ~3 × 10⁹). Additionally, the analysis of BLUEs has turned out to be particularly complex due to the abundance of radiation belt particles (at high latitudes and in the South Atlantic Anomaly [SAA]) and cosmic rays all over the planet. True BLUEs can not be fully distinguished from radiation belt particles and cosmic rays unless other ground-based measurements associated with the optically detected BLUEs are available. Thus, the search algorithm of BLUEs presented in Soler et al. (2021), <https://doi.org/10.1029/2021gl094657> is now completed with a new additional step that, if used, can considerably smooth the SAA shadow but can also underestimate the number of BLUEs worldwide.

Plain Language Summary The presence of corona electrical discharges in thunderclouds has been suspected for a long time. These thunderstorm coronas can be observed as Blue Luminous Events (BLUEs) formed by a large number of streamers characterized by their distinct 337 nm light flashes with absent (or negligible) 777.4 nm component (typical of lightning leaders). The Modular Multispectral Imaging Array of the Atmosphere-Space Interaction Monitor has successfully allowed us to map and characterize BLUEs. The results presented here include a global analysis of key properties of BLUEs such as their characteristic rise times and duration, their depth with respect to cloud tops, vertical length and number of streamers. This study also includes two different global annual average climatologies of BLUEs depending on considerations about the rise time and total duration of BLUEs worldwide.

1. Introduction

Radio, optical, and some indirect chemical recordings since the early 1980s suggest that cold, non-thermal streamer corona discharges are common in thunderstorms worldwide (Bandara et al., 2019; Bozem et al., 2014; Le Vine, 1980; Li et al., 2021; Liu et al., 2018; Neubert et al., 2021; Soler et al., 2020; Wiens et al., 2008). Fast breakdown (Rison et al., 2016; Tilles et al., 2019) seems to underlie streamer coronas that cause the so-called Narrow Bipolar Events (NBEs) originally detected by Le Vine (1980) in the form of strong Very High Frequency sources from in-cloud discharges.

Typical light spectra of streamer corona discharges in air are strongly dominated by near-ultraviolet blue emissions (300–450 nm) corresponding to the Second Positive System (SPS) of molecular nitrogen (N₂) (Ebert et al., 2010; Gallimberti et al., 1974; Grum & Costa, 1976) with the strongest transition at 337 nm (Gordillo-Vázquez et al., 2012; Hoder et al., 2016; Malagón-Romero & Luque, 2019) and generally undetectable oxygen atom 777.4 nm emissions typical of lightning. Optical signals from lightning stroke flashes are characterized by including both 337 nm emissions and, especially, strong 777.4 nm optical emissions (Blakeslee et al., 2020; Christian

Methodology: S. Soler, F. J. Gordillo-Vázquez, F. J. Pérez-Invernón, O. Chanrion, N. Østgaard
Project Administration: F. J. Gordillo-Vázquez
Resources: F. J. Gordillo-Vázquez
Software: S. Soler
Supervision: F. J. Gordillo-Vázquez
Validation: S. Soler, F. J. Gordillo-Vázquez
Visualization: S. Soler, F. J. Gordillo-Vázquez
Writing – original draft: F. J. Gordillo-Vázquez
Writing – review & editing: F. J. Gordillo-Vázquez

et al., 1989, 2003; Montanyà et al., 2021). However, BLUEs exhibit strong optical emissions in the 337 nm and negligible (at the noise level) 777.4 nm emissions (Soler et al., 2020). Corona streamers can appear alone as leaderless corona discharges and/or in combination with hot leaders of lightning, blue jets (Wescott et al., 1995) and blue starters (Edens, 2011; Wescott et al., 1996).

The term Blue LUMinous Events (BLUEs) has been recently applied to in-cloud and to partially emerged transient electrical discharges that emit pulses of light mostly blue, that is, they could include a small fraction of red (from the first positive system of N₂) and infrared optical emissions (777.4 nm from atomic oxygen). This definition includes blue jets and starters, but also positive and negative NBEs, which are the VLF/LF radio manifestation of in-cloud leaderless streamer coronas (Cooray et al., 2020; C. Kuo et al., 2015; Li et al., 2021; Liu et al., 2018, 2019; Neubert et al., 2021; Rison et al., 2016; Soler et al., 2020; Tilles et al., 2019). Apart from distinct optical emissions directly associated with corona streamers, the dissimilarity between BLUEs and lightning discharges is also manifested by the fact that BLUEs can occur individually with no associated lightning discharges or they can be the initial event of lightning discharges (Li et al., 2022; López et al., 2022; Soler et al., 2020, 2021).

BLUEs optical detections from space have been reported from the limb-pointing Imager of Sprites/Upper Atmospheric Lightning onboard FORMOSAT-2 (J. Chou et al., 2011; J.-K. Chou et al., 2018; C.-L. Kuo et al., 2005; C. Kuo et al., 2015;; Liu et al., 2018). A variety of BLUEs including kilometer-scale blue discharges at the cloud top layer at ~18 km altitude, blue starters and a pulsating blue jet propagating into the stratosphere were color photographed from the International Space Station (ISS) (Chanrion et al., 2017). BLUEs have also been recently observed by the nadir-pointing MMIA onboard ASIM in the ISS since April 2018 (Husbjerg et al., 2022; Li et al., 2021; Neubert et al., 2021; Soler et al., 2020). However, it is a known issue that powerful NBEs are highly likely to be misclassified or simply missed by lightning locating systems (Zhu et al., 2022). For 1022 NBEs reported by Leal et al. (2019), the misclassification rates were 78% and 56% for the National Lightning Detection Network (NLDN–GLD360) and the Earth Network Total Lightning Network, respectively. They also found that the percentage of misclassified NBEs becomes even higher for higher intensity events. Connected to this, Chanrion et al. (2017) saw BLUEs from the ISS without any GLD360 detections. Thus, ground based detection of BLUEs by lightning networks remains a challenge.

A number of recent thunderstorm case-based works have detailed studied properties of BLUEs associated with positive NBEs (Soler et al., 2020), negative NBEs (Li et al., 2021; Liu, Zhu, et al., 2021; Liu, Lu, et al., 2021; Neubert et al., 2021) and multiple pulse BLUEs (Li et al., 2022) using MMIA data of thunderclouds in several locations of the world. Additionally, a recent study presented the first worldwide nighttime climatology of BLUEs in thunderclouds derived from 2 years of BLUEs data recorded by MMIA in ASIM (Soler et al., 2021).

Here we focus on analyzing key properties of worldwide nighttime BLUEs detected by MMIA between 1 April 2019 and 31 March 2021 (note that ASIM can only observe during the night). Our study also discusses BLUEs depending on considerations about the rise time and total duration of BLUEs in the planet. We investigate intrinsic properties of BLUE events including temporal features like pulse shape (single, multiple or irregular), rise times and total duration times. We analyze the 337 nm Peak Power Density (PPD) and total brightness, and the depth below thundercloud tops where BLUEs occur as a function of the latitude and longitude. Finally, we also present worldwide zonal and meridional distributions for the vertical lengths and approximate number of streamers of single pulse BLUEs.

2. Observations and Data

Observations of BLUEs were carried out with the MMIA high sampling rate (100 k samples/s) photometers in the near UV (337 nm/4 nm), tuned to the strongest line of the N₂ SPS, and in the near infrared band (777.4 nm/5 nm) for recording the atomic oxygen triplet line of lightning. MMIA also incorporates a high-speed photometer in the UV (180–230 nm), capable of recording part of the N₂ Lyman–Birge–Hopfield band, and a pair of 337 nm/4 nm and 777.4 nm/5 nm filtered cameras (at 12 fps) with ~400 m/pixel spatial resolution (Chanrion et al., 2019).

BLUEs exhibit strong features in the 337 nm/4 nm photometer with negligible (or very minor) signal in the 777.4 nm/5 nm photometer, which is continuously monitored (Soler et al., 2020). Once a true positive BLUE detection is confirmed, the cameras are checked for possible associated images.

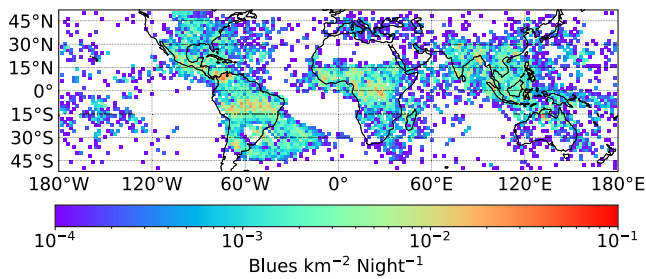


Figure 1. Two-year average (1 April 2019 through 31 March 2021) nighttime climatology of global Blue Luminous Events (BLUE) electrical activity in thunderclouds (GD-1) showing ~46,000 BLUEs. The map is generated using $2^\circ \times 2^\circ$ grid cells. The BLUEs shown can have any temporal shape, that is, no distinction has been made here among BLUEs with a single (impulsive or not) pulse, multiple pulses or any other irregular pulse shape. The annual global rate of GD-1 BLUEs peak at $9.5 \text{ events s}^{-1}$ in the local midnight (00.00 local solar time), and show a decreasing global rate as local daytime approaches (and there is less Modular Multispectral Imaging Array observation time). On average, the global annual average rate of BLUEs in GD-1 is $6.0 \text{ events s}^{-1}$. Note that Atmosphere-Space Interaction Monitor can only observe during the night.

old” (Soler et al., 2021), and with the criterion on how the total duration of an event is calculated (from the fitted signal) getting the position in a time of the blue peak and then go backward and forward until the signal drops below 10% of the maximum.

When our algorithm searches for a BLUE event it needs to find at least five counts above the threshold, so apparently, we can assume that all events should last at least $50 \mu\text{s}$. However, when we apply these criteria to very sharp BLUEs with a high Peak Power Density we can see that, in some cases, the total time can be less than $50 \mu\text{s}$ (as mentioned above).

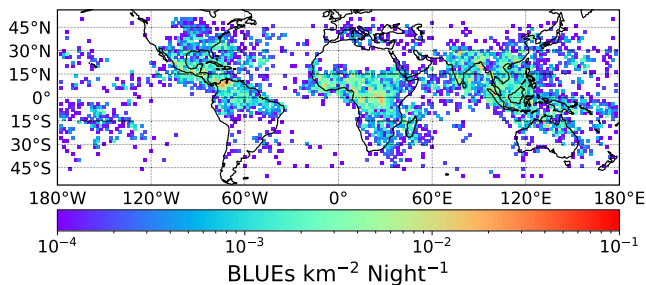


Figure 2. Two-year average (1 April 2019 through 31 March 2021) nighttime climatology of global Blue Luminous Events (BLUE) electrical activity in thunderclouds (GD-2) removing events in all planets (including the South Atlantic Anomaly) with rise time ($\tau_{\text{rise}} \leq 40 \mu\text{s}$) and total duration ($\tau_{\text{total}} \leq 150 \mu\text{s}$). The map is generated using $2^\circ \times 2^\circ$ grid cells. Note that it is quite possible that not all the removed ~20,000 events with respect to GD-1 are radiation belt particles and cosmic rays. Consequently, the number of BLUEs (~26,500) shown in this GD-2 distribution is most probably underestimated. The BLUEs shown can have any temporal shape, that is, no distinction has been made here among BLUEs with a single (impulsive or not) pulse, multiple pulses, or any other irregular pulse shape. The annual global rate of GD-2 BLUEs peak at $5.5 \text{ events s}^{-1}$ in the local midnight (00.00 local solar time), and show a decreasing global rate as local daytime approaches (and there is less Modular Multispectral Imaging Array observation time). On average, the global annual average rate of BLUEs in GD-2 is $3.5 \text{ events s}^{-1}$. Note that Atmosphere-Space Interaction Monitor can only observe during the night.

The two worldwide annual average distributions of nighttime BLUEs presented and discussed here (see Figures 1 and 2) were obtained with global ASIM-MMIA level 1 (calibrated) data in a period of two years (1 April 2019–31 March 2021) shifted 7 months ahead (see Section 4 for details) with respect to the earlier 2-year period explored in Soler et al. (2021). The BLUEs shown in Figures 1 and 2 can have any temporal shape, that is, no distinction has been made here among BLUEs with a single (impulsive or not) pulse, multiple pulses or any other irregular pulse shape. The first global average distribution (GD-1) of BLUEs presented was derived using the algorithm described in Soler et al. (2021).

In order to explore the possible influence of Radiation Belt Particles (RBP) and Cosmic Rays (CR) on our dataset, the second global average distribution (GD-2) of nighttime BLUEs discussed here includes the condition that 337 nm events are removed in the entire planet when their rise times (τ_{rise}) are $\leq 40 \mu\text{s}$ and their total duration (τ_{total}) times are $\leq 150 \mu\text{s}$ (see Figure 2). This is a new (optional) step in the Soler et al. (2021) algorithm that by default allows events with any duration above $50 \mu\text{s}$. In spite of this, there are still some hundreds of BLUEs with duration below $50 \mu\text{s}$ (see GD-2 in the right column of Figures 10 and 11). This is fully compatible with point 4 of our BLUE search algorithm that reads “create groups defined by five or more consecutive blue counts ($10 \mu\text{s}$ each) above the 337 nm photometer thresh-

old” (Soler et al., 2021), and with the criterion on how the total duration of an event is calculated (from the fitted signal) getting the position in a time of the blue peak and then go backward and forward until the signal drops below 10% of the maximum.

It is worth mentioning here that ultrahigh energy ($>10^{19} \text{ eV}$) CRs are being monitored from the ISS by the nadir-facing Multiwavelength Imaging New Instrument for the Extreme Universe Space Observatory (Mini-EUSO) telescope in operation since October 2019 (Bacholle et al., 2021; Miyamoto et al., 2021). Mini-EUSO observes the nighttime Earth in the near ultraviolet (UV) - blue range (290 – 430 nm), with a spatial resolution of about 6.3 km (FOV of $300 \times 300 \text{ km}$) and a temporal resolution of $2.5 \mu\text{s}$. According to Mini-EUSO observations, ultrahigh energy CRs cross one or a few pixels of the photocathode detector releasing a high-intensity light curve that can last a maximum of $\leq 150 \mu\text{s}$ with a sharp increase ($\leq 40 \mu\text{s}$) (see figure 5 in Miyamoto et al. [2021]).

The global distributions of nighttime BLUEs in Figures 1 and 2 include ~46,000 events and 26,500 events, respectively. One can note that it is then quite possible that not all the ~20,000 events removed in GD-2 with respect to GD-1 are RBPs and CRs. The presence of the South Atlantic Anomaly (SAA) can be distinguished within a rectangle with borders in latitudes 5°S and 45°S , and longitudes 0° and 100°W in Figure 1 for GD-1. Note that the SAA’s shadow is mostly removed in Figure 2 for GD-2 but with the drawback of probable underestimation of the number of BLUEs worldwide in GD-2.

The seasonal nighttime average distributions of BLUEs according to GD-1 and GD-2 are further shown in Figures 3 and 4, respectively. In both seasonal distributions, BLUEs are more common in the boreal summer closely followed by the boreal autumn. The main visual difference between Figures 1

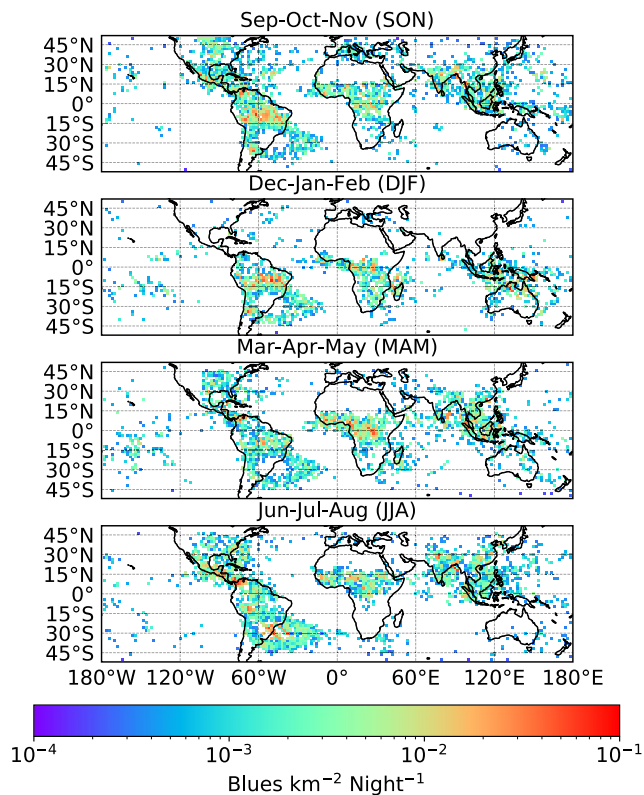


Figure 3. Nighttime seasonal distribution of Blue Luminous Events (BLUE) electrical activity in thunderclouds associated to GD-1 in Figure 1. The global nighttime seasonal BLUE rates are: 6.7 (SON), 4.7 (DJF), 5.9 (MAM), and 6.8 (JJA) BLUEs s^{-1} . These maps are generated using $2^\circ \times 2^\circ$ grid cells. The BLUEs shown can have any temporal shape, that is, no distinction has been made here among BLUEs with a single (impulsive or not) pulse, multiple pulses or any other irregular pulse shape.

coefficient (Soler et al., 2020). For short times after the optical emission and assuming that the mean absorption time (τ_A) of the photons inside the cloud is much larger than τ_D , the fit discussed in Li et al. (2021) predicts a $\sim(\tau_D t)^{-1/2}$ dependence for the photon flux exiting the cloud top. From N and τ_D one can obtain the number of streamers in the BLUE as well as its maximum length L_0 (Li et al., 2021) (for more details, see the Supporting Information S1).

We have assumed that extended sources are located in the perfect nadir (no angle with vertical). However, this might not always be the case and such an assumption could underestimate the total optical energy of all the 337 nm photons emitted by a BLUE.

Finally, we found that $\sim 2,700$ events (with $R^2 > 0.75$) in GD-1 and ~ 262 events (with $R^2 > 0.75$) in GD-2 can be fit by both the point-like and the extended-source models (see Table 1). Likely these are cases where the optical source is both small and close to the cloud top.

Table 1 shows the total number of BLUE events in GD-1 and GD-2 discriminating according to their type (point-like or extended). Note that for the point-like sources the total time is derived from the FHT model fitting, while for the extended sources the total time is obtained from the raw data (since the fitting used for the extended sources does not include the rise).

and 3, and the distributions of BLUEs in Soler et al. (2021) is the disappearance of events occurring in high latitudes during the annual average and during the SON, DJF, and MAM.

3. Methodology

The key features of the BLUEs were obtained by applying different types of fits (depending on whether the light source is considered point-like [see Figure S1 of the Supporting Information S1] or extended [see Figure S2 of the Supporting Information S1]) to the impulsive 337 nm light curves among the $\sim 46,000$ and $\sim 26,500$ BLUEs registered worldwide according to the global annual average distributions shown in Figures 1 and 2. However, as commented below, the two types of fits considered here are valid provided that the 337 nm light curve of the BLUEs exhibits a relatively clear (single pulse) impulsive shape, which occurs in only $\sim 12\%$ and $\sim 10\%$ of the $\sim 46,000$ and $\sim 26,500$ BLUEs detected by MMIA in the investigated period (1 April 2019–31 March 2021) and distributed according to GD-1 and GD-2, respectively. Clear impulsive single pulse BLUEs are considered when the fittings have $R^2 > 0.75$, being R^2 the so-called coefficient of determination (used as a metric of fit goodness), which can change between negative values and 1 (perfect fit). A number of correlations have been established between the above mentioned characteristics of BLUEs.

By assuming a point-like source for the light source deep in the cloud, the first hitting time (FHT) fit (Soler et al., 2020) provides a first approximation to the single pulse BLUE depth with respect to cloud tops within thunderstorms, 337 nm peak power density (and total brightness), rise and total times (Luque et al., 2020; Soler et al., 2020).

The tail of the light curve from an extended source (see Figure S2 of the Supporting Information S1) that spans altitudes close to the cloud top to a maximum distance L_0 inside the cloud can also be fitted to obtain the best-fit cutoff (characteristic photon diffusion) time $\tau_D = L_0^2/4D$, and the total number of source photons (N) (Li et al., 2021), with D being a diffusion

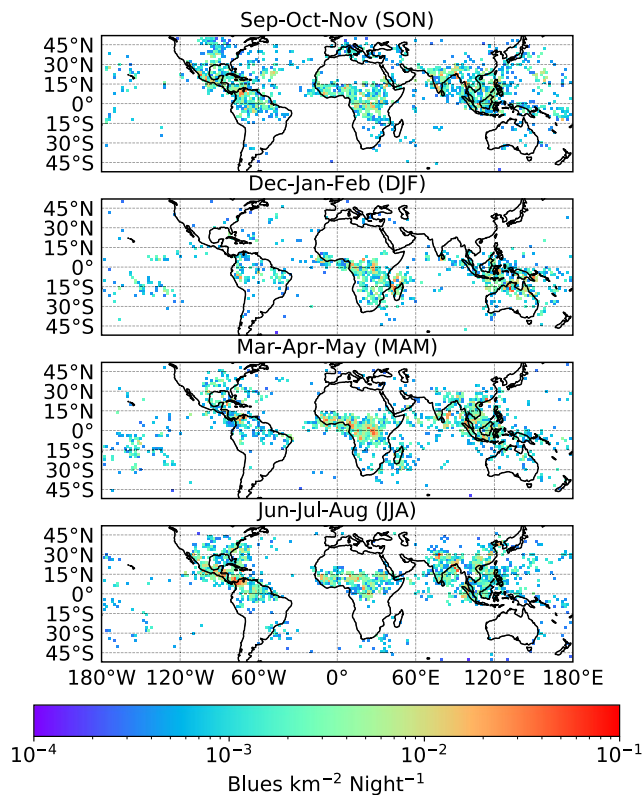


Figure 4. Nighttime seasonal distribution of Blue Luminous Events (BLUE) electrical activity in thunderclouds associated to GD-2 in Figure 2. The global nighttime seasonal BLUE rates are: 3.7 (SON), 2.6 (DJF), 3.7 (MAM), and 4.0 (JJA) BLUEs s⁻¹. These maps are generated using 2° × 2° grid cells. The BLUEs shown can have any temporal shape, that is, no distinction has been made here among BLUEs with a single (impulsive or not) pulse, multiple pulses or any other irregular pulse shape.

4.1. Distribution of BLUEs According to Altitude and Peak Power Density

The worldwide distribution of BLUE altitudes in terms of latitude is displayed in Figures 7a and 7c for GD-1 and (b, d) for GD-2. All panels in Figures 7 and 8 except panels (c, d) of Figure 7 display 5,374 (GD-1) BLUE events (~12% of ~46,000) and 2,242 (GD-2) BLUE events (~10% of ~26,500) with good quality fitting ($R^2 > 0.75$), that is, those that are closest to impulsive single pulse point-like sources. However, panels (c, d) of Figure 7 shows most of the ~46,000 BLUEs of GD-1 (panel (c)) and ~26,500 BLUEs of GD-2 (panel (d)) detected by ASIM-MMIA that is fittable independently of the fitting quality, that is, for any value of R^2 . Thus, Figure 7 (c, d) shows the altitude distribution of BLUE events which 337 nm light curves might not be fully explained by single pulse point-like sources.

4. Results and Discussion

In order to provide some perspective to the reader, Figures 5 and 6 show four maps that display, in four intervals of peak power density (PPD), the geographical distribution (per 2° × 2° grid cell) of the ~46,000 and ~26,500 BLUEs detected by ASIM-MMIA corresponding to the GD-1 and GD-2 annual average distributions. Panels (a), (b), (c), and (d) of Figures 5 and 6 show BLUEs with PPD <25 μWm⁻², between ≥25 and 50 μWm⁻², between ≥50 and 100 μWm⁻², and ≥100 μWm⁻², respectively.

In regard to the ~53,000 BLUEs earlier reported by Soler et al. (2021), there are 3183 with PPD ≥100 μWm⁻². Of these 3,183 and 2,992 events, that is, ~94% (mostly in latitudes above 35°N and below 35°S) concentrate between 1 September 2018 and 31 March 2019 during the first 7 months of the 2-year period evaluated by Soler et al. (2021), while in the following 17 months there are only ~6% of the 3,183 BLUEs worldwide with PPD >100 μWm⁻². Interestingly, we only found 282 BLUEs with PPD >100 μWm⁻² when searching (with exactly the same algorithm as in Soler et al. [2021]) in the two years 1 April 2019–31 March 2021.

It is important to note that on March 2019 there was an update of the ASIM-MMIA cosmic ray rejection algorithm software (ON only over the SAA before March 2019, ON everywhere after March 2019) that could have influenced the above findings.

The trend described above for the PPD ≥100 μWm⁻² range is also identified (using exactly the same algorithm as in Soler et al. [2021]) in the other three lower PPD ranges between 1 September 2018 and 31 March 2019. However, the difference in the number of BLUEs (relative importance) of each PDD range with respect to successive periods of 7 months (1 September 2019–31 March 2020, and 1 September 2020–31 March 2021) is ~6%.

Consequently, in our study, we decided to move forward 7 months the period of time chosen to carry out the analysis of characteristics of BLUEs presented here.

Table 1
Total Number of BLUE Events in GD-1 and GD-2 Discriminating According to Their Type (Point-Like or Extended)

	GD-2	
	GD-1	Eliminate events worldwide with ($\tau_{rise} \leq 40 \mu s$ and $\tau_{total} \leq 150 \mu s$)
TOTAL	46,283	26,355
Point-like source ($R^2 > 0.75$)	5,374	2,242
Extended source ($R^2 > 0.75$)	4,258	553
Common ($R^2 > 0.75$)	2,717	262

Note. That for the Point-Like Sources the Total Time Is Derived From the First Hitting Time (FHT) Model Fitting, While for the Extended Sources the Total Time Is Obtained From the Raw Data.

The approximate altitude distributions of BLUEs (see Figure 7 a–d) are derived by assuming that the global cloud top height distribution can be approximated by the annual mean variation of the tropopause heights with the latitude (Heumesser et al., 2021; Offroy et al., 2015). BLUEs can, however, occur associated with deep convection scenarios and are often detected in overshooting cloud tops extending across the local tropopause (Liu et al., 2018), which would break down the above-mentioned assumption and can introduce an altitude uncertainty of ~1–3 km (Liu et al., 2018).

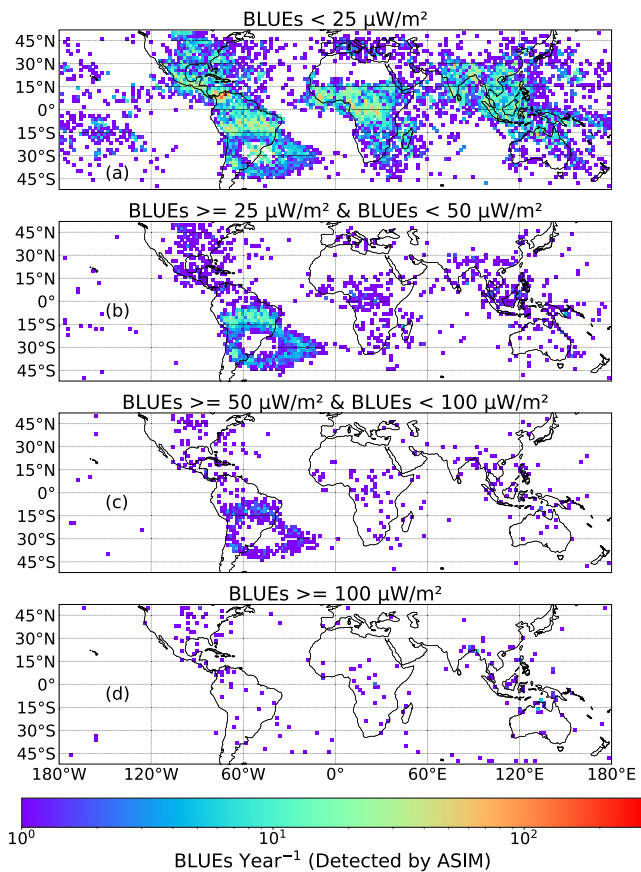


Figure 5. Geographical distribution (in $2^\circ \times 2^\circ$ grid cells) of the $\sim 46,000$ nighttime GD-1 Blue Luminous Events (BLUEs) detected by Atmosphere-Space Interaction Monitor-Modular Multispectral Imaging Array in the two-year period from 1 April 2019 to 31 March 2021. Panels (a), (b), (c) and (d) show BLUEs of any shape with peak power density (PPD) between ≥ 3 and $< 25 \mu\text{Wm}^{-2}$, between ≥ 25 and $< 50 \mu\text{Wm}^{-2}$, between ≥ 50 and $< 100 \mu\text{Wm}^{-2}$, and $\geq 100 \mu\text{Wm}^{-2}$, respectively. There are 39,980 BLUEs in panel (a) (19990/year), 4,367 in panel (b) (2,183.5/year), 833 in panel (c) (416.5/year), and 282 in panel (d) (141/year). The BLUEs shown in these maps can have any temporal shape, that is, no distinction has been made here among BLUEs with a single (impulsive or not) pulse, multiple pulses or any other irregular pulse shape.

Figures 7e, 7f and 8 show detailed GD-1 (left column) and GD-2 (right column) latitudinal and longitudinal distributions of impulsive single pulse BLUEs with their peak power density (μWm^{-2}). Large ($\geq 50 \mu\text{Wm}^{-2}$) peak power BLUE events appear scattered across all latitudes and longitudes. Most single pulse BLUEs exhibit peak power densities $< 25 \mu\text{Wm}^{-2}$ (as shown in Figures 5 and 6 for BLUEs with all sorts of pulse shapes).

BLUEs with peak power densities below $25 \mu\text{Wm}^{-2}$ are common within the tropics, within the Indian subcontinent, and near the ocean of the Asia/Australia BLUE chimney. The three BLUE chimneys appear in the meridional distribution of BLUEs shown in panels (c) through (f) of Figure 8.

In order to compare and/or validate the geographical (Figure 2) and altitude (Figures 7b, 7d) distributions of BLUEs obtained in this paper for GD-2 we compared them (see Figure S17 and Figure S18 of the Supporting Information S1) with several case-based studies of BLUEs already published (provided the events occurred within the dates of our climatology). Figure S17 of Supporting Information S1 shows local maps with numbers 1, 2, 3, and 4 on them indicating the centroid of the set of BLUEs investigated in the case-based studies reported in (a) Li et al. (2021) and Liu, Lu, Neubert, et al. (2021) over Southern China, (b) López et al. (2022) over Colombia, (c) Soler et al. (2020) over Indonesia, and (d) the study by Li et al. (2022) about multiple pulse BLUEs over nearby Malaysia. The numbers 1 through 4 in Figure S18 in Supporting Information S1 are placed in the mean altitude and in the centroid (in terms of latitude and longitude) of the reported BLUE events in the mentioned local studies. A number with a ' indicates the mean height obtained by radio (VLF/LF) for the same set of BLUE events. The red dashed lines (above and below the solid red line) indicate the ± 3 km uncertainty associated with our approximation to globally compute the tropopause in each latitude. It can be seen that strong thunderstorms with overshooting tops penetrating into the lower stratosphere (cases 1 and 4) can create some discrepancies between the heights obtained by optical (applied globally in our analysis) and radio but, in any case, within the uncertainty of the method chosen to represent the tropopause at a global scale.

The red line in panels (a)–(d) in Figure 7 marks the annual mean variation of the tropopause heights with latitude. Two zonal layers of BLUEs (see greenish zones) can be distinguished: a top layer of shallow BLUEs (≤ 0.5 km depth), and a deeper (2.5–5 km depth) layer of BLUEs mostly located among tropical latitudes (10°S to 20°N).

Figures 7e, 7f and Figure 8 show detailed GD-1 (left column) and GD-2 (right column) latitudinal and longitudinal distributions of impulsive single pulse BLUEs with respect to their different depths below thundercloud tops around the globe and peak power densities. A thin and shallow layer of BLUEs at a depth ≤ 1 km below cloud tops is visible across all latitudes (see Figures 7e and 7f). This usually corresponds to the location of negative NBEs (Li et al., 2021; Wu et al., 2014). A second thicker and deeper layer between ~ 1.25 km and ~ 3.25 km below thundercloud tops is also distinguishable within the tropics and part of the subtropical regions (Figures 7e and 7f). The longitudinal distributions of depths clearly exhibit three BLUE chimneys (see Figures 8c and 8d) with the American chimney in GD-1 (see Figure 8c) being more populated due to the South America's contribution. A fourth dim chimney is also visible in the Pacific Ocean. These changes in GD-2 where the most populated chimney is Asia/Australia (see Figure 8d) and with the Pacific chimney remaining.

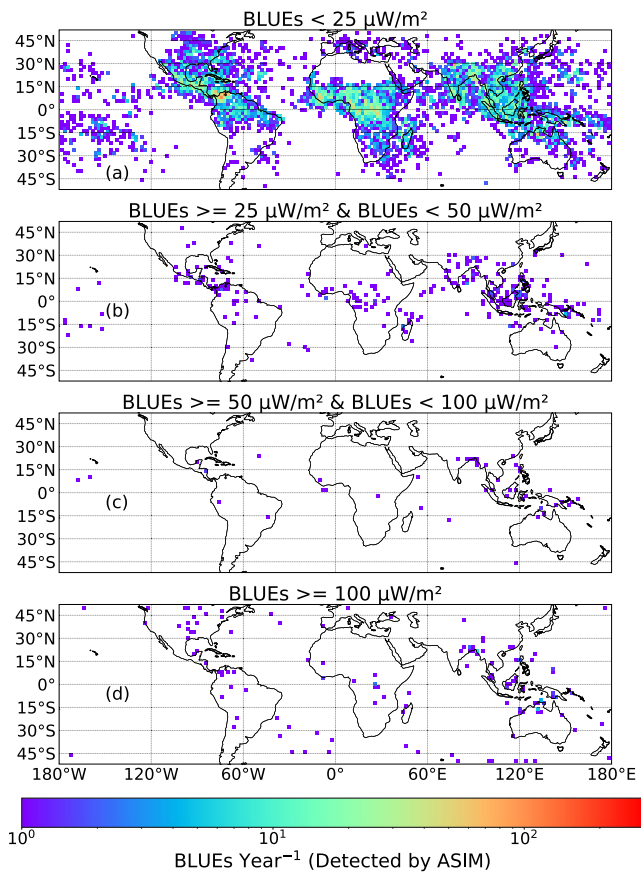


Figure 6. Geographical distribution (in $2^\circ \times 2^\circ$ grid cells) of the $\sim 26,500$ nighttime GD-2 Blue Luminous Events (BLUEs) detected by Atmosphere-Space Interaction Monitor-Modular Multispectral Imaging Array in the two-year period from 1 April 2019 to 31 March 2021 removing events in all the planet (including the SAA) with rise time ($\tau_{rise} \leq 40 \mu s$) and total duration ($\tau_{total} \leq 150 \mu s$). Panels (a), (b), (c), and (d) show BLUEs of any shape with peak power density (PPD) between ≥ 3 and $< 25 \mu W m^{-2}$, between ≥ 25 and $< 50 \mu W m^{-2}$, between ≥ 50 and $< 100 \mu W m^{-2}$, and $\geq 100 \mu W m^{-2}$, respectively. There are 25,720 BLUEs in panel (a) (12,860/year), 380 in panel (b) (190/year), 52 in panel (c) (26/year), and 204 in panel (d) (102/year). The BLUEs shown in these maps can have any temporal shape, that is, no distinction has been made here among BLUEs with a single (impulsive or not) pulse, multiple pulses or any other irregular pulse shape.

4.2. Global Distribution of BLUEs According to Rise and Total Times

Figure 9 presents zonal (a)-(d) and meridional (e)-(h) distributions of the rise and total duration times of impulsive single pulse BLUEs of GD-1 [left column] and GD-2 [right column]), respectively. Note that the rise and total times are calculated as the elapsed times since the raw (or fitted) signal is above 10% of the maximum until it reaches the maximum (rise time), and until it passes the maximum and decreases again to 10% of the maximum (total time). For point-like sources, the rise and total time are derived from the FHT model fitting, while for extended sources the total time is obtained from the raw data. The presence of the SAA can be clearly seen between $5^\circ S$ and $20^\circ S$ in panels (a, c) of Figure 9 for GD-1, and between 0° and $100^\circ W$ in panels (e, g) of Figure 9 for GD-1.

Single pulse BLUEs with fast ($\leq 30 \mu s$) rise times and short (≤ 0.5 ms) total times occur across all latitudes and longitudes. Zonal distributions show that the single pulse BLUEs concentrated within the tropics exhibit rise and total times ranging from $50 \mu s$ to 0.5 ms, and from 0.8 ms to ~ 4 ms, respectively. Complementarily, meridional distributions displayed in Figures 9e and 9h show that single pulse BLUEs in the three main chimneys exhibit roughly the same rise and total duration times with the Europe/Africa chimney being the one with slightly faster and shorter rise times and durations.

The left/right columns of Figure 10 for GD-1/GD-2 show the connection between the peak power density ($\mu W m^{-2}$) and total brightness ($\mu W m m^{-2}$) of impulsive single pulse BLUEs and their rise and total duration times. Both magnitudes (peak power density and maximum brightness) exhibit two clear populations. The most numerous population includes single pulse BLUEs with fast ($\leq 50 \mu s$) rise times and short (≤ 0.5 ms) durations reaching peak powers and total brightnesses of up to 200 and $30\text{--}40 \mu W m m^{-2}$, respectively. The second group of single pulse BLUEs reaches longer rise times (up to ~ 0.8 ms) and total times (up to ~ 4 ms) associated with lower peak powers ($\leq 50 \mu W m^{-2}$) and total brightnesses ($\sim 25 \mu W m m^{-2}$). The two groups of BLUEs with fast ($\leq 50 \mu s$) and slow ($> 50 \mu s$ and up to $\sim 0.8\text{--}1.0$ ms) rise times are consistent with those mentioned in Husbjerg et al. (2022).

4.3. Correlations Between BLUE's Depth and Their Rise and Total Times

The left/right columns of Figure 11 for GD-1/GD-2 represent how light scattering affects key features (rise time and total time) of the 337 nm light curves of BLUEs. In order to appropriately visualize the relationships between the rise and total times we have plotted the total and rise times as a function of the depth below the cloud top (panels (a, c) for GD-1 and (b, d) for GD-2), and the total time versus rise time for GD-1 (panel (e)) and for GD-2 (panel (f)).

In general, the closer the BLUE source is to the cloud top, the faster rise times and shorter duration times due to the weak scattering (as reported by Li et al. [2021]). On the contrary, when BLUE sources are deeply buried in storm clouds (like the ones in Soler et al. [2020]), scattering by cloud droplets and ice crystals blurs their image as observed from above and produced 337 nm light curves characterized by relatively long rise times ($0.2\text{--}0.5$ ms) and total duration times (> 1.5 ms). Therefore, shallow (≤ 1 km depth) single pulse BLUEs exhibit fast rise times below $\sim 50 \mu s$ and total duration times below ~ 0.5 ms. Deeper single pulse BLUEs occurring between ~ 1 and ~ 4 km below cloud tops are characterized by rise and total times that increase up to about 0.8 ms (for 4 km) and 5 ms (for ~ 3 km), respectively. The bottom branch of Figure 11a and 11c for GD-1 also shows some few BLUEs that, even occurring deeper ($1\text{--}8$ km below cloud tops) in thunderclouds, still exhibit fast rise times of $\leq 60 \mu s$ and

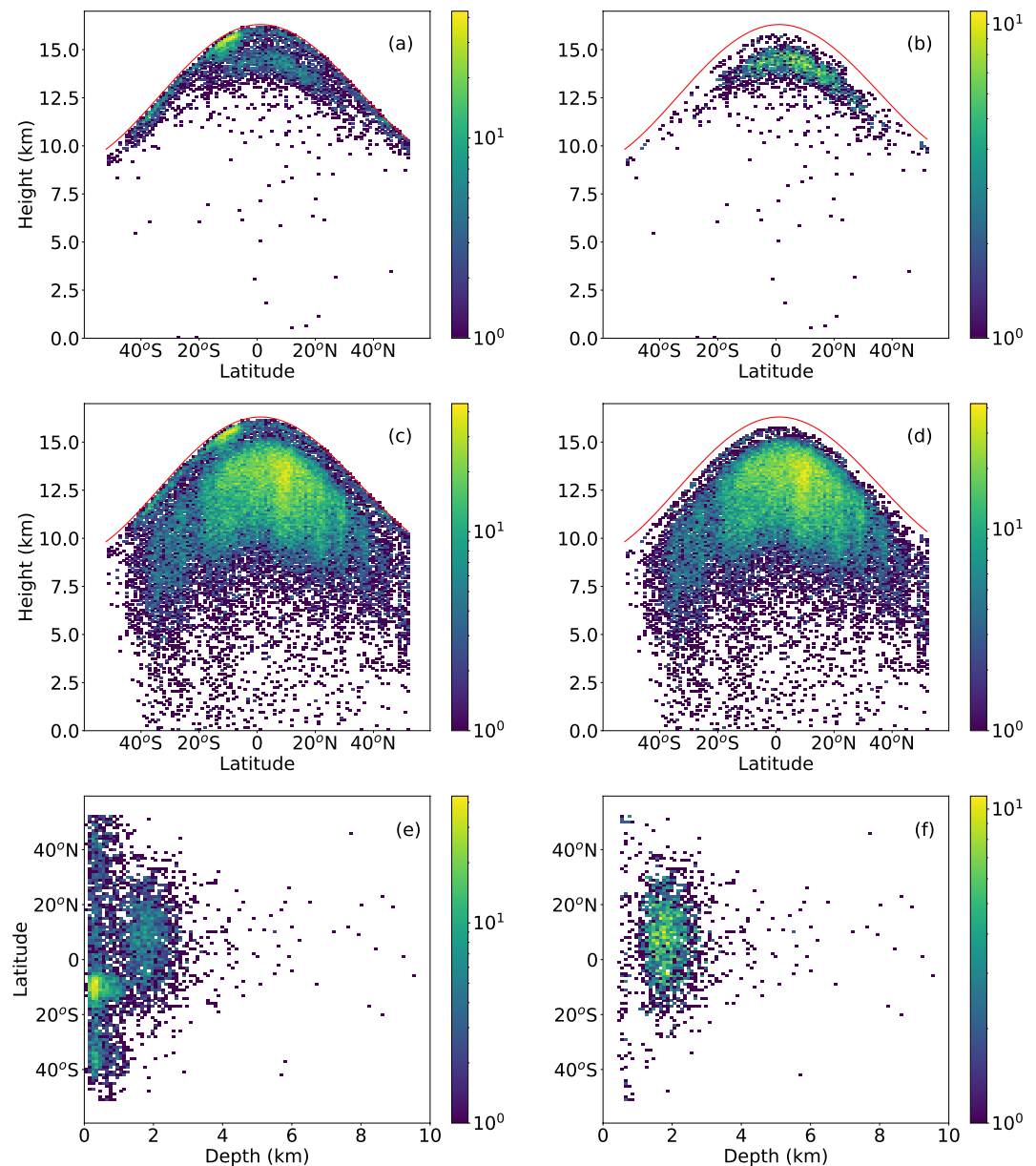


Figure 7. Approximate altitude distributions of GD-1 (left column) and GD-2 (right column) impulsive single pulse Blue Luminous Events (BLUEs) (with $R^2 > 0.75$) (a), (b), all sort of first hitting time (FHT) fittable BLUEs in GD-1 and GD-2 with any value of R^2 (c), (d). Zonal distributions of GD-1 and GD-2 impulsive single pulse BLUE depths (e), (f). Note that, always, GD-1 is in the left column and GD-2 is in the right column. The colorbar indicates number of events.

short durations ($\leq 200 \mu\text{s}$). This result is not physically possible and should be disregarded. These few unphysical events in Figure 11a, 11c for GD-1 disappear almost completely in Figures 11b, 11d for GD-2.

Figure 11 (e) for GD-1 and Figure 11f for GD-2 show the connection between the total time duration of single pulse BLUEs and their rise time. For fast ($\leq 40 \mu\text{s}$) rise times, the total duration ranges from ~ 100 to $\sim 300 \mu\text{s}$. However, as the rise time increases beyond $\sim 40 \mu\text{s}$, panels (e, f) of Figure 11 show the main branch in the top associated with single pulse BLUEs with relatively long (0.4–5 ms) total durations.

It is also interesting to note that, as shown in panels (a) for GD-1 and (b) for GD-2 of Figure 10, fast ($\leq 40 \mu\text{s}$) rise time BLUEs come with a 337 peak power density that can reach values of up to $\sim 200 \mu\text{Wm}^{-2}$. When rise times are beyond $50 \mu\text{s}$ the BLUEs' peak power density stays below $\sim 50 \mu\text{Wm}^{-2}$ and exhibits a decreasing trend as rise time increases from ~ 0.1 ms to ~ 1 ms.

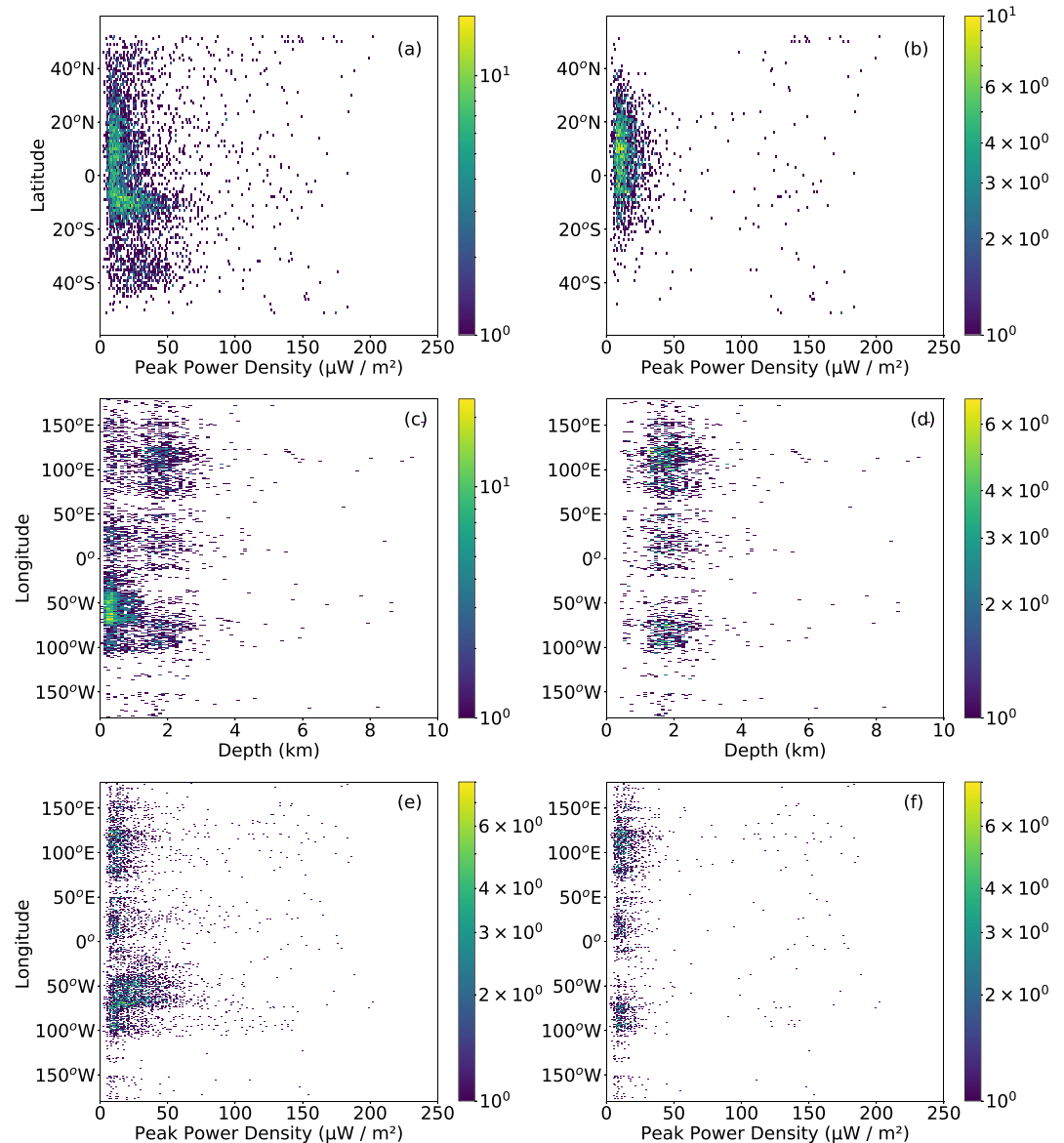


Figure 8. Zonal distributions of GD-1 and GD-2 impulsive single pulse Blue Luminous Events (BLUE) peak power density (a), (b). Meridional distributions of impulsive single pulse BLUE depths (c), (d) and peak power density (e), (f). Note that, always, GD-1 is in the left column and GD-2 is in the right column. The colorbar indicates number of events.

4.4. Global Zonal/Meridional Distributions of BLUEs' Streamers and Lengths

Figure 12 presents the zonal and meridional distributions of the lengths (L_0) and the number of streamers (k) for GD-1 (left column) and GD-2 (right column) of single pulse BLUEs, respectively. The lengths of most single pulse BLUEs roughly vary between ~ 100 and $\sim 1,500$ m in GD-1 (see panels (a) and (c) in Figure 12). However, the group of tropical BLUEs with lengths between 2 km and up to ~ 5 km dominate in GD-2 (see panels (b) and (d) in Figure 12).

According to our analysis, the number of streamers in single pulse BLUEs ranges between 10^8 and 10^9 in agreement with previous results (Cooray et al., 2020; Li et al., 2021; Liu et al., 2019). BLUEs with most streamers concentrate between 20°S and 20°N (see panels (e) for GD-1 and (f) for GD-2 of Figure 12) with the tropical band including some BLUEs with up to $\sim 2\text{--}3 \times 10^9$ streamers. The meridional distribution of BLUEs' streamers (see panels (g) for GD-1 and (h) for GD-2 of Figure 12) exhibits a three chimney structure with the Asia/Australia chimney including some BLUEs with up to $\sim 2\text{--}3 \times 10^9$ streamers.

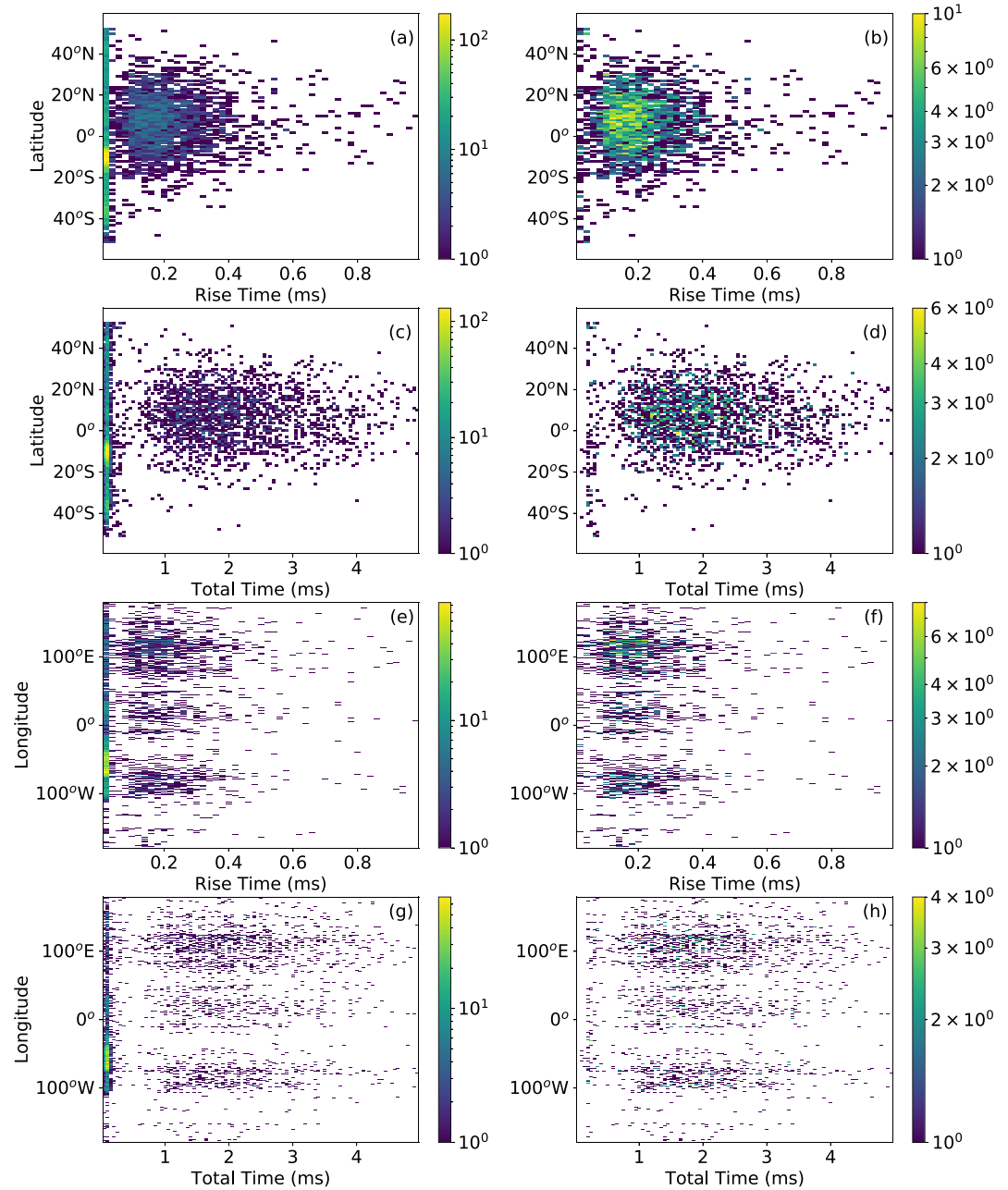


Figure 9. Zonal (a)–(d) and meridional (e)–(h) distributions of rising times (a, b, e, f) and total times (duration) (c, d, g, h) of impulsive single pulse BLUES in GD-1 (left column) and GD-2 (right column). Note that, always, GD-1 is in the left column and GD-2 is in the right column. The colorbar indicates number of events.

5. Conclusions

We have found in this study that approximately ~10% to ~12% of all BLUES detected globally are impulsive single pulse ones. However, there can still be ambiguous (mostly not impulsive) single pulse events with $R^2 < 0.75$. A systematic analysis has been undertaken to determine the geographical (zonal and meridional) distribution of key properties of BLUES including impulsive single pulse ones. In particular, our analysis focused on quantifying their altitudes and depths below thundercloud tops, characteristic rise and total duration times, peak power density, total brightness, vertical extension, and number of streamers.

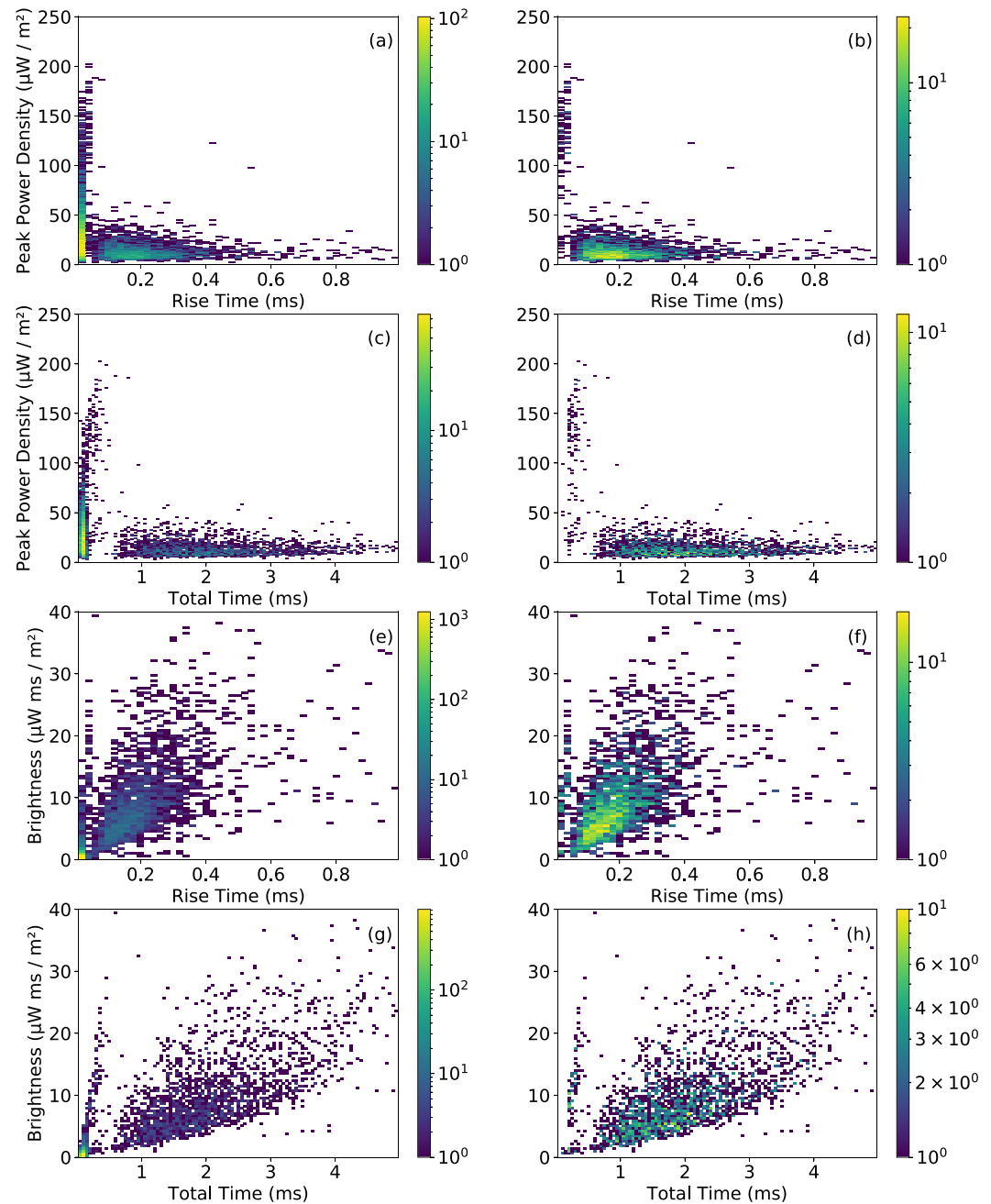


Figure 10. Variation of the peak power density (a)–(d) and total brightness (e)–(h) as a function of the GD-1 (left column) and GD-2 (right column) impulsive single pulse Blue Luminous Events (BLUE) rise times (a, b, e, f) and total time (duration) (c, d, g, h). Note that the rise and total times are calculated as the elapsed times since the raw signal is above 10% of the maximum until it reaches the maximum (rise time), and until it passes the maximum and decreases again to 10% of the maximum (total time). Note that, always, GD-1 is in the left column and GD-2 is in the right column. The colorbar indicates number of events.

Our study concludes that the over detection (concentrated between 1 September 2018 and 31 March 2019) of BLUEs shown in Soler et al. (2021) in the high latitudes of the northern and southern hemispheres was caused by a combined effect of (a) an update in the ASIM-MMIA cosmic rejection algorithm software (ON only over the SAA before March 2019, ON everywhere after March 2019) and (b) cosmic rays and the particle flux from the inner radiation belts detectable in the SAA and in the high latitudes of the northern and southern hemispheres.

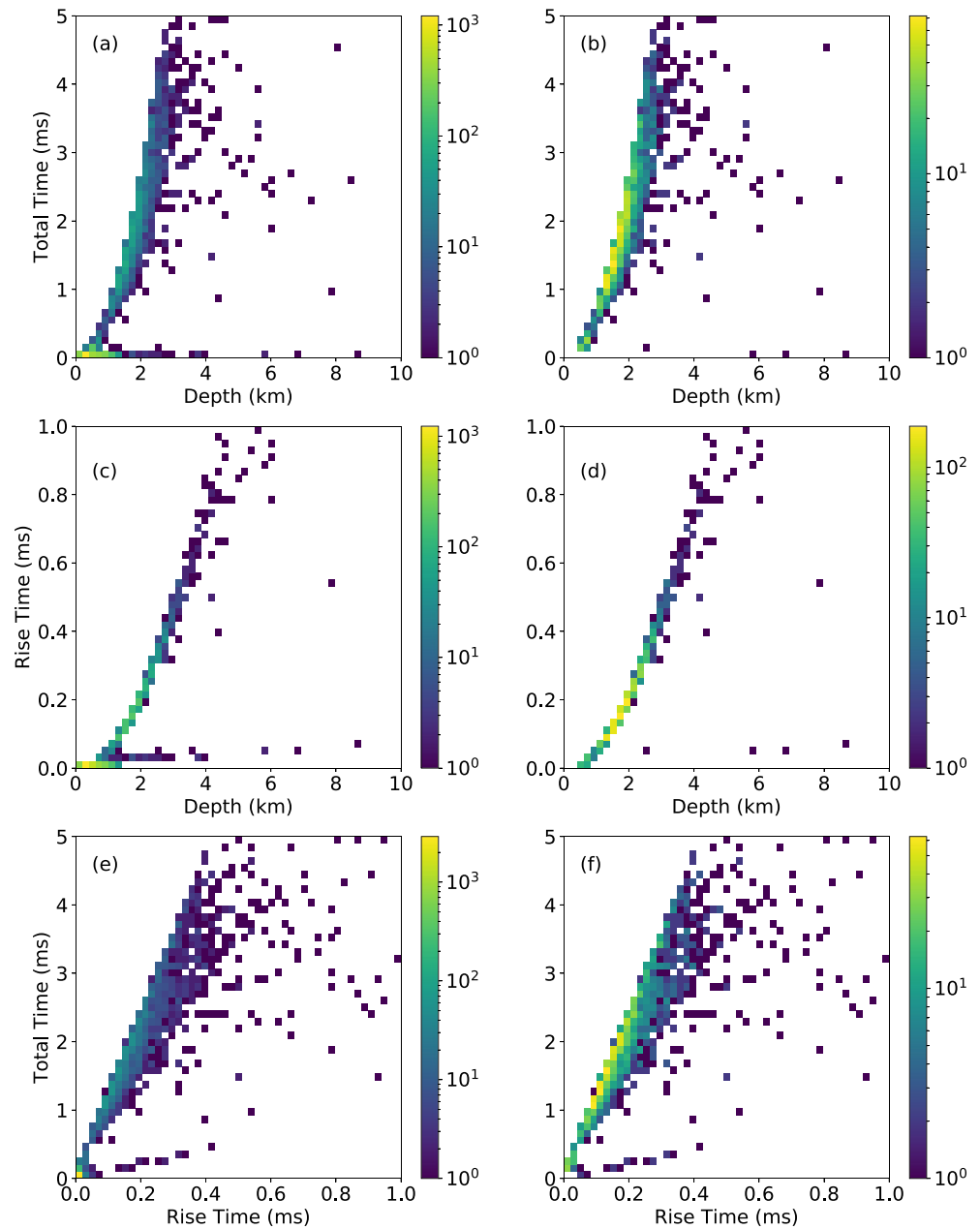


Figure 11. Total times (duration) and rise times of impulsive single pulse Blue Luminous Events (BLUES) in GD-1 (left column) and GD-2 (right column) as a function of depth (a)–(d). Panels (e) and (f) show the relationship between total times (duration) and rise times for GD-1 (left column) and GD-2 (right column). Note that panels (a), (c) of GD-1 show the presence of some few unphysical events located deep (1–8 km below cloud tops) in thunderclouds characterized by simultaneously exhibiting very short total times ($\leq 200 \mu\text{s}$) and rise times ($\leq 60 \mu\text{s}$). This is mostly solved in panels (b), (d) of GD-2. Note that, always, GD-1 is in the left column and GD-2 is in the right column. The colorbar indicates number of events.

As a consequence of this, two new worldwide annual average (and seasonal) distributions of nighttime BLUES were generated and presented here using global ASIM-MMIA level 1 (calibrated) data in a different 2-year period (1 April 2019–31 March 2021) shifted 7 months ahead with respect to the earlier 2-year period explored in Soler et al. (2021). While the first global average distribution (GD-1) of BLUES is derived using exactly the same algorithm described in Soler et al. (2021), the second distribution (GD-2) removes events in all planets (including the SAA) with rise time ($\tau_{\text{rise}} \leq 40 \mu\text{s}$) and total duration ($\tau_{\text{total}} \leq 150 \mu\text{s}$). This remarkably removes the SAA shadow

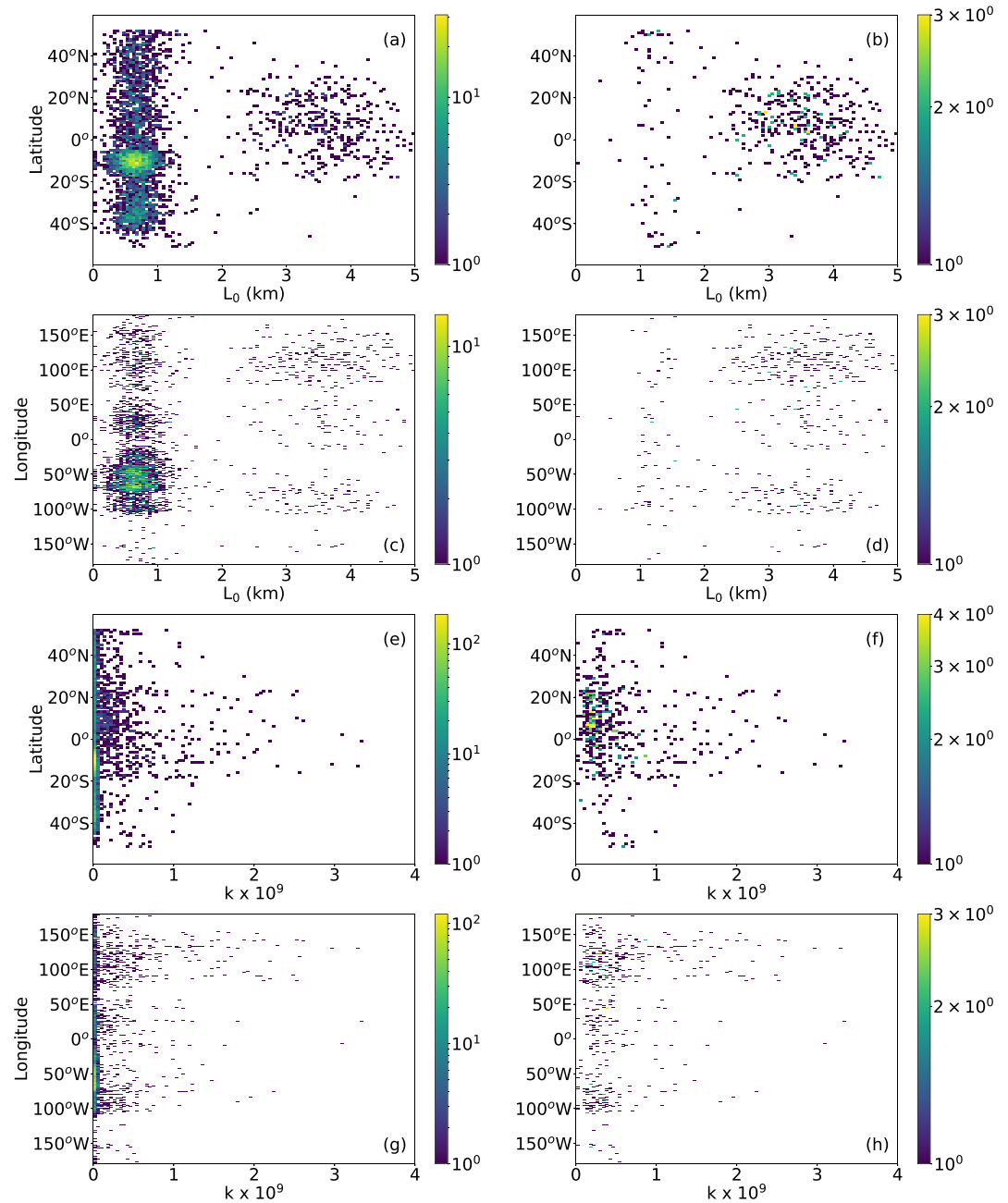


Figure 12. Zonal and meridional distributions of the lengths (L_0) (a)–(d) and number of streamers ($k \times 10^9$) (e)–(h) of impulsive single pulse Blue Luminous Events in GD-1 (left column) and GD-2 (right column). Note that, always, GD-1 is in the left column and GD-2 is in the right column. The colorbar indicates number of events.

in GD-1 but can also underestimate the number of BLUEs in South America and, consequently, the total number of BLUEs that could range between the $\sim 26,500$ obtained for GD-2 and the $\sim 46,000$ counted for GD-1.

Two distinct populations of BLUEs with peak power density $< 25 \mu\text{Wm}^{-2}$ (common) and $\geq 25 \mu\text{Wm}^{-2}$ (rare) are observed. While BLUEs with small to moderate ($< 25 \mu\text{Wm}^{-2}$) peak power can occur over land and the maritime regions, BLUEs with large ($> 50 \mu\text{Wm}^{-2}$) peak power occur scattered across all latitudes and longitudes mainly over land.

BLUEs are globally found between the cloud tops and ~ 4 km below cloud tops in the tropics and ≤ 1 km in mid and higher latitudes. Fast rise time (< 0.05 ms) BLUEs with short (< 0.5 – 0.6 ms) total times occur (across

all latitudes and longitudes) very superficially (<1 km) near cloud tops with high power density $\geq 100 \mu\text{Wm}^{-2}$. BLUEs with peak powers below $50 \mu\text{Wm}^{-2}$ have longer (>50 μs) rise times and longer (>0.5 ms) durations.

Zonal distributions show that BLUEs concentrated within the tropics exhibit rise and total times ranging from 50 μs up to 0.5 ms, and from 0.8 ms up to ~ 4 ms, respectively. Complementarily, meridional distributions show that BLUEs in the three chimneys exhibit roughly the same rise and total duration times with the Europe/Africa chimney being the one with slightly faster rise times and shorter durations.

The vertical length of BLUEs as well as their number of streamers are two interesting features of in-cloud corona discharges that have also been characterized and geographically analyzed in this work. The vertical extension of most impulsive single pulse BLUEs changes between ~ 100 and $\sim 1,500$ m with a group of longer (up to ~ 4 –5 km) BLUEs located within the tropics in the three main BLUE chimneys especially visible in GD-2.

The obtained climatology for the features of BLUEs opens the door to investigating the relationship between the characteristics of BLUEs and meteorological parameters. The observed variability in some features of BLUEs, such as their depth, number of streamers, rise time and the total duration of their optical pulses, indicates that they can be influenced by some meteorological parameters like the convective available potential energy (see Figure S12 in the Supplementary Material of Soler et al. [2021] and Husbjerg et al. [2022]). These findings suggest that monitoring the occurrence and the features of BLUEs could serve as an indicator to characterize severe weather (deep convection episodes) (Husbjerg et al., 2022; Liu et al., 2018; Soler et al., 2021). In particular, Husbjerg et al. (2022) show the difference in convection levels for lightning-producing storms and BLUE-producing storms.

Recent airborne observations (Brune et al., 2021) and laboratory experimental results (Jenkins et al., 2021) indicate that considerable amounts of oxidant species (OH, HO₂) could be directly produced by visible and subvisible (corona) electrical discharges in thunderstorm anvils and not only be the indirect result of atmospheric chemical processes after the injection of lightning NO_x (Finney et al., 2016; Gordillo-Vázquez et al., 2019; Schumann & Huntrieser, 2007). The production of OH and HO₂ recently reported by Jenkins et al. (2021) could also be due to air plasma streamers in corona discharges occurring in thunderstorm anvils (Bozem et al., 2014; Gordillo-Vázquez & Pérez-Invernón, 2021; Minschwaner et al., 2008; Pérez-Invernón et al., 2019; Zahn et al., 2002) since thundercloud coronas (Li et al., 2021; Liu, Lu, Neubert, et al., 2021; Soler et al., 2020) are now known to be more frequent (about 10 per s worldwide) (Soler et al., 2021) than previously suspected. Corona discharges in thunderclouds are especially frequent in the Tornado alley in North America (Soler et al., 2021) where airborne observations by Brune et al. (2021) have recently reported significant regional transient enhancements of OH and HO₂ concentrations during thundercloud electrical activity.

In summary, the geographical (and seasonal) distributions of BLUEs and all their characteristics presented here (including the knowledge of the altitude distribution of impulsive single pulse BLUEs and their number of streamers) can be critical parameters to explore how corona discharges in thunderclouds could contribute to the global chemical budget of important oxidant species like OH and HO₂, and key greenhouse gases such as ozone (O₃) and nitrous oxide (N₂O) in the climate-sensitive region of the upper troposphere and lower stratosphere region.

Acknowledgments

ASIM is a mission of ESA's SciSpace programme for scientific utilization of the ISS and non-ISS space exploration platforms and space environment analogues. ASIM and the ASIM Science Data Centre are funded by ESA and by national grants of Denmark, Norway, and Spain. This work was supported by the Spanish Ministry of Science and Innovation under project PID2019-109269RB-C43 and the FEDER program. SS acknowledges a PhD research contract through the project PID2019-109269RB-C43. FJPI acknowledges the sponsorship provided by Junta de Andalucía under Grant POSTDOC-21-00052. AL and DL were supported by the European Research Council (ERC) under European Union H2020 programme/ERC grant agreement 681257. SS, FJGV, AL, and DL acknowledge financial support from the State Agency for Research of the Spanish MCIU through the "Center of Excellence Severo Ochoa" award for the Instituto de Astrofísica de Andalucía (SEV-2017-0709).

Data Availability Statement

ASIM level 1 data are proprietary and cannot be publicly released at this stage. Interested parties should direct their request to the ASIM Facility Science Team (FST). ASIM data request can be submitted through: <https://asdc.space.dtu.dk> by sending a message to the electronic address <mailto:asdc@space.dtu.dk>.

References

- Bacholle, S., Barrillon, P., Battisti, M., Belov, A., Bertaina, M., Bisconti, F., et al. (2021). Mini-euso mission to study Earth uv emissions on board the iss. *The Astrophysical Journal - Supplement Series*, 253(2), 36. <https://doi.org/10.3847/1538-4365/abd93d>
- Bandara, S., Marshall, T., Karunarathne, S., Karunarathne, N., Siedlecki, R., & Stolzenburg, M. (2019). Characterizing three types of negative narrow bipolar events in thunderstorms. *Atmospheric Research*, 227, 263–279. <https://doi.org/10.1016/j.atmosres.2019.05.013>
- Blakeslee, R. J., Lang, T. J., Koshak, W. J., Buechler, D., Gatlin, P., Mach, D. M., et al., (2020). Three years of the lightning imaging sensor onboard the international space station: Expanded global coverage and enhanced applications. *Journal of Geophysical Research: Atmospheres*, 125(16), e2020JD032918. <https://doi.org/10.1029/2020jd032918>
- Bozem, H., Fischer, H., Gurk, C., Schiller, C., Parchatka, U., Koenigstedt, R., et al. (2014). Influence of corona discharge on the ozone budget in the tropical free troposphere: A case study of deep convection during gabriel. *Atmospheric Chemistry and Physics*, 14(17), 8917–8931. <https://doi.org/10.5194/acp-14-8917-2014>

- Brune, W., McFarland, P., Bruning, E., Waugh, S., MacGorman, D., Miller, D., et al. (2021). Extreme oxidant amounts produced by lightning in storm clouds. *Science*, 372(6543), 711–715. <https://doi.org/10.1126/science.abg0492>
- Chanrion, O., Neubert, T., Mogensen, A., Yair, Y., Stendel, M., Singh, R., & Siingh, D. (2017). Profuse activity of blue electrical discharges at the tops of thunderstorms. *Geophysical Research Letters*, 44(1), 496–503. <https://doi.org/10.1002/2016gl071311>
- Chanrion, O., Neubert, T., Rasmussen, I. L., Stoltze, C., Tcherniak, D., Jessen, N. C., et al. (2019). The modular multispectral imaging array (MMIA) of the ASIM payload on the international space station. *Space Science Reviews*, 215(4), 28. <https://doi.org/10.1007/s11214-019-0593-y>
- Chou, J., Tsai, L., Kuo, C., Lee, Y., Chen, C., Chen, A., et al. (2011). Optical emissions and behaviors of the blue starters, blue jets, and gigantic jets observed in the Taiwan transient luminous event ground campaign. *Journal of Geophysical Research*, 116(A7). <https://doi.org/10.1029/2010ja016162>
- Chou, J.-K., Hsu, R.-R., Su, H.-T., Chen, A. B.-C., Kuo, C.-L., Huang, S.-M., et al. (2018). Isual-observed blue luminous events: The associated sferics. *Journal of Geophysical Research: Space Physics*, 123(4), 3063–3077. <https://doi.org/10.1002/2017ja024793>
- Christian, H. J., Blakeslee, R. J., Boccippio, D. J., Boeck, W. L., Buechler, D. E., Driscoll, K. T., et al. (2003). Global frequency and distribution of lightning as observed from space by the Optical Transient Detector. *Journal of Geophysical Research*, 108(D1), 4005. <https://doi.org/10.1029/2002jd002347>
- Christian, H. J., Blakeslee, R. J., & Goodman, S. J. (1989). The detection of lightning from geostationary orbit. *Journal of Geophysical Research*, 94(D11), 13329–13337. <https://doi.org/10.1029/jd094id11p13329>
- Cooray, V., Cooray, G., Rubinstein, M., & Rachidi, F. (2020). Modeling compact intracloud discharge (CID) as a streamer burst. *Atmosphere*, 11(5), 549. <https://doi.org/10.3390/atmos11050549>
- Ebert, U., Nijdam, S., Li, C., Luque, A., Briels, T., & van Veldhuizen, E. (2010). Review of recent results on streamer discharges and discussion of their relevance for sprites and lightning. *Journal Geophysical Research*, 115(A7), A00E43. <https://doi.org/10.1029/2009JA014867>
- Edens, H. (2011). Photographic and lightning mapping observations of a blue starter over a new Mexico thunderstorm. *Geophysical Research Letters*, 38(17). <https://doi.org/10.1029/2011gl048543>
- Finney, D., Doherty, R., Wild, O., & Abraham, N. L. (2016). The impact of lightning on tropospheric ozone chemistry using a new global lightning parametrisation. *Atmospheric Chemistry and Physics*, 16(12), 7507–7522. <https://doi.org/10.5194/acp-16-7507-2016>
- Gallimberti, I., Hepworth, J. K., & Klewe, R. C. (1974). Spectroscopic investigation of impulse corona discharges. *Journal of Physics D*, 7(6), 880–898. <https://doi.org/10.1088/0022-3727/7/6/315>
- Gordillo-Vázquez, F. J., Luque, A., & Simek, M. (2012). Near infrared and ultraviolet spectra of TLEs. *Journal of Geophysical Research*, 117(A5), A05329. <https://doi.org/10.1029/2012ja017516>
- Gordillo-Vázquez, F. J., & Pérez-Invernón, F. J. (2021). *A review of the impact of transient luminous events on the atmospheric chemistry: Past, present, and future*. Atmospheric Research. 105432.
- Gordillo-Vázquez, F. J., Pérez-Invernón, F. J., Huntrieser, H., & Smith, A. (2019). Comparison of six lightning parameterizations in CAM5 and the impact on global atmospheric chemistry. *Earth and Space Science*, 6(12), 2317–2346. <https://doi.org/10.1029/2019ea000873>
- Grum, F., & Costa, L. (1976). Spectral emission of corona discharges. *Applied Optics*, 15(1), 76–79. <https://doi.org/10.1364/ao.15.000076>
- Heumesser, M., Chanrion, O., Neubert, T., Christian, H. J., Dimitriadou, K., Gordillo-Vázquez, F. J., et al. (2021). Spectral observations of optical emissions associated with terrestrial gamma-ray flashes. *Geophysical Research Letters*, 48(4), 2020GL090700. <https://doi.org/10.1029/2020gl090700>
- Hoder, T., Simek, M., Bonaventura, Z., Prukner, V., & Gordillo-Vázquez, F. J. (2016). Radially and temporally resolved electric field of positive streamers in air and modelling of the induced plasma chemistry. *Plasma Sources Science and Technology*, 25(4), 045021. <https://doi.org/10.1088/0963-0252/25/4/045021>
- Husbjerg, L. S., Neubert, T., Chanrion, O., Dimitriadou, K., Li, D., Stendel, M., et al. (2022). Observations of blue corona discharges in thunderclouds. *Geophysical Research Letters*, 49(12), e2022GL099064. <https://doi.org/10.1029/2022gl099064>
- Jenkins, J. M., Brune, W. H., & Miller, D. O. (2021). Electrical discharges produce prodigious amounts of hydroxyl and hydroperoxyl radicals. *Journal of Geophysical Research: Atmospheres*, 126(9), e2021JD034557. <https://doi.org/10.1029/2021jd034557>
- Kuo, C., Su, H., & Hsu, R. (2015). The blue luminous events observed by ISUAL payload on board FORMOSAT-2 satellite. *Journal of Geophysical Research: Space Physics*, 120(11), 9795–9804. <https://doi.org/10.1002/2015ja021386>
- Kuo, C.-L., Hsu, R. R., Chen, A. B., Su, H. T., Lee, L. C., Mende, S. B., et al. (2005). Electric fields and electron energies inferred from the ISUAL recorded sprites. *Geophysical Research Letters*, 32(19), L19103. <https://doi.org/10.1029/2005GL023389>
- Leal, A. F., Rakov, V. A., & Rocha, B. R. (2019). Compact intracloud discharges: New classification of field waveforms and identification by lightning locating systems. *Electric Power Systems Research*, 173, 251–262. <https://doi.org/10.1016/j.epsr.2019.04.016>
- Le Vine, D. M. (1980). Sources of the strongest rf radiation from lightning. *Journal of Geophysical Research*, 85(C7), 4091–4095. <https://doi.org/10.1029/jc085ic07p04091>
- Li, D., Luque, A., Gordillo-Vázquez, F. J., Liu, F., Lu, G., Neubert, T., et al. (2021). Blue flashes as counterparts to narrow bipolar events: The optical signal of shallow in-cloud discharges. *Journal of Geophysical Research: Atmospheres*, 126(13), e2021JD035013. <https://doi.org/10.1029/2021jd035013>
- Li, D., Luque, A., Lehtinen, N. G., Gordillo-Vázquez, F., Neubert, T., Lu, G., et al. (2022). Multi-pulse corona discharges in thunderclouds observed in optical and radio bands. *Geophysical Research Letters*, 49(13), e2022GL098938. <https://doi.org/10.1029/2022gl098938>
- Liu, B., Zhu, B., Lu, G., Lu, G., Lei, J., Shao, J., et al. (2021). Meteorological and electrical conditions of two mid-latitude thunderstorms producing blue discharges. *Journal of Geophysical Research: Atmospheres*, 126, (8), e2020JD033648. <https://doi.org/10.1029/2020jd033648>
- Liu, F., Lu, G., Neubert, T., Lei, J., Chanrion, O., Østgaard, N., et al. (2021). Optical emissions associated with narrow bipolar events from thunderstorm clouds penetrating into the stratosphere. *Nature Communications*, 12(1), 1–8. <https://doi.org/10.1038/s41467-021-26914-4>
- Liu, F., Zhu, B., Lu, G., Qin, Z., Lei, J., Peng, K.-M., et al. (2018). Observations of blue discharges associated with negative narrow bipolar events in active deep convection. *Geophysical Research Letters*, 45(6), 2842–2851. <https://doi.org/10.1002/2017gl076207>
- Liu, N., Dwyer, J. R., Tilles, J. N., Stanley, M. A., Krehbiel, P. R., Rison, W., et al. (2019). Understanding the radio spectrum of thunderstorm narrow bipolar events. *Journal of Geophysical Research: Atmospheres*, 124(17–18), 10134–10153. <https://doi.org/10.1029/2019jd030439>
- López, J. A., Montanyà, J., van der Velde, O., Romero, D., Gordillo-Vázquez, F. J., Pérez-Invernón, F. J., et al. (2022). Initiation of lightning flashes simultaneously observed from space and the ground: Narrow bipolar events. *Atmospheric Research*, 268, 105981. <https://doi.org/10.1016/j.atmosres.2021.105981>
- Luque, A., Gordillo-Vázquez, F. J., Li, D., Malagón-Romero, A., Pérez-Invernón, F. J., Schmalzried, A., et al. (2020). Modeling lightning observations from space-based platforms (cloudscat. jl 1.0). *Geoscientific Model Development*, 13(11), 5549–5566. <https://doi.org/10.5194/gmd-13-5549-2020>
- Malagón-Romero, A., & Luque, A. (2019). Spontaneous emergence of space stems ahead of negative leaders in lightning and long sparks. *Geophysical Research Letters*, 46(7), 4029–4038. <https://doi.org/10.1029/2019gl082063>

- Minschwaner, K., Kalnajs, L., Dubey, M., Avallone, L., Sawaengphokai, P., Edens, H., & Winn, W. (2008). Observation of enhanced ozone in an electrically active storm over Socorro, NM: Implications for ozone production from corona discharges. *Journal of Geophysical Research*, *113*(D17), D17208. <https://doi.org/10.1029/2007jd009500>
- Miyamoto, H., Fenu, F., Barghini, D., Battisti, M., Belov, A., Bertaina, M., et al. others (2021). Simulations studies for the mini-euso detector. arXiv preprint arXiv:2112.12150.
- Montanyà, J., López, J. A., Morales Rodríguez, C. A., van der Velde, O. A., Fabró, F., Pineda, N., et al., others (2021). A simultaneous observation of lightning by asim, Colombia-lightning mapping array, glm, and iss-lis. *Journal of Geophysical Research: Atmospheres*, *126*(6), e2020JD033735. <https://doi.org/10.1029/2020jd033735>
- Neubert, T., Chanrion, O., Heumesser, M., Dimitriadou, K., Husbjerg, L., Rasmussen, I. L., et al. (2021). Observation of the onset of a blue jet into the stratosphere. *Nature*, *589*(7842), 371–375. <https://doi.org/10.1038/s41586-020-03122-6>
- Offroy, M., Farges, T., Kuo, C. L., Chen, A. B.-C., Hsu, R.-R., Su, H.-T., et al. (2015). Temporal and radiometric statistics on lightning flashes observed from space with the isual spectrophotometer. *Journal of Geophysical Research: Atmospheres*, *120*(15), 7586–7598. <https://doi.org/10.1002/2015jd023263>
- Pérez-Invernón, F. J., Gordillo-Vázquez, F. J., Smith, A. K., Arnone, E., & Winkler, H. (2019). Global occurrence and chemical impact of stratospheric Blue Jets modeled with WACCM4. *Journal of Geophysical Research: Atmospheres*, *124*(5), 2841–2864. <https://doi.org/10.1029/2018JD029593>
- Rison, W., Krehbiel, P. R., Stock, M. G., Edens, H. E., Shao, X.-M., Thomas, R. J., et al. (2016). Observations of narrow bipolar events reveal how lightning is initiated in thunderstorms. *Nature Communications*, *7*(1), 10721. <https://doi.org/10.1038/ncomms10721>
- Schumann, U., & Huntrieser, H. (2007). The global lightning-induced nitrogen oxides source. *Atmospheric Chemistry and Physics*, *7*(14), 3823–3907. <https://doi.org/10.5194/acp-7-3823-2007>
- Soler, S., Gordillo-Vázquez, F., Pérez-Invernón, F., Luque, A., Li, D., Neubert, T., et al. (2021). Global frequency and geographical distribution of nighttime streamer corona discharges (blues) in thunderclouds. *Geophysical Research Letters*, *48*(18), e2021GL094657. <https://doi.org/10.1029/2021gl094657>
- Soler, S., Pérez-Invernón, F. J., Gordillo-Vázquez, F. J., Luque, A., Li, D., Malagón-Romero, A., et al. (2020). Blue optical observations of narrow bipolar events by ASIM suggest corona streamer activity in thunderstorms. *Journal of Geophysical Research: Atmospheres*, *125*(16), e2020JD032708. <https://doi.org/10.1029/2020jd032708>
- Tilles, J. N., Liu, N., Stanley, M. A., Krehbiel, P. R., Rison, W., Stock, M. G., et al. (2019). Fast negative breakdown in thunderstorms. *Nature Communications*, *10*(1), 1648. <https://doi.org/10.1038/s41467-019-09621-z>
- Wescott, E. M., Sentman, D., Osborne, D., Hampton, D., & Heavner, M. (1995). Preliminary results from the Sprites94 aircraft campaign: 2. Blue jets. *Geophysical Research Letters*, *22*(10), 1209–1212. <https://doi.org/10.1029/95GL00582>
- Wescott, E. M., Sentman, D. D., Heavner, M. J., Hampton, D. L., Osborne, D. L., & Vaughan, O. H. (1996). Blue starters: Brief upward discharges from an intense Arkansas thunderstorm. *Geophysical Research Letters*, *23*(16), 2153–2156. <https://doi.org/10.1029/96GL01969>
- Wiens, K. C., Hamlin, T., Harlin, J., & Suszcynsky, D. M. (2008). Relationships among narrow bipolar events, “total” lightning, and radar-inferred convective strength in Great Plains thunderstorms. *Journal of Geophysical Research*, *113*(D5). <https://doi.org/10.1029/2007jd009400>
- Wu, T., Yoshida, S., Ushio, T., Kawasaki, Z., & Wang, D. (2014). Lightning-initiator type of narrow bipolar events and their subsequent pulse trains. *Journal of Geophysical Research: Atmospheres*, *119*(12), 7425–7438. <https://doi.org/10.1002/2014jd021842>
- Zahn, A., Brenninkmeijer, C., Crutzen, P., Parrish, D., Sueper, D., Heinrich, G., & Heintzenberg, J. (2002). Electrical discharge source for tropospheric “ozone-rich transients”. *Journal of Geophysical Research*, *107*(D22), 4638. ACH-16. <https://doi.org/10.1029/2002jd002345>
- Zhu, Y., Stock, M., Lapierre, J., & DiGangi, E. (2022). Upgrades of the Earth networks total lightning network in 2021. *Remote Sensing*, *14*(9), 2209. <https://doi.org/10.3390/rs14092209>